

Y3.N21/518/933

for Aeronautics

MAILED

FEB 29 1940

To Library, ...

Hartford Public

m933

TECHNICAL MEMORANDUMS
NATIONAL ADVISORY COMMITTEE FOR AERONAUTICS

No. 933

THE STRENGTH OF SHELL AND TUBULAR SPAR WINGS

By H. Ebner

Luftfahrtforschung
Vol. 14, Nos. 4/5, April 20, 1937
Verlag von R. Oldenbourg, München und Berlin

Washington
February 1940

NATIONAL ADVISORY COMMITTEE FOR AERONAUTICS

TECHNICAL MEMORANDUM NO. 933

THE STRENGTH OF SHELL AND TUBULAR SPAR WINGS*

By H. Ebner

The following is a survey of the strength problems arising on shell and tubular spar wings. The treatment of the shell wing strength is primarily confined to those questions which concern the shell wing only; those pertaining to both shell wing and shell body together have already been treated in another report (reference 1, T.M. No. 838). The discussion of stress condition and compressive strength of shell wings and tubular spar wings is prefaced by several considerations concerning the spar and shell design of metal wings from the point of view of strength.

I. SPAR AND SHELL DESIGN FOR METAL WINGS

1. Characteristics and Design of Spar and Shell Wings

On the wings and bodies of earlier airplanes, the support of the skin on the carrying of bending and torsional loads was, as a rule, wholly disclaimed. Subsequently, the metal or plywood covering served as shear-resistant bond for the transverse loads and the twisting moments as well as to provide the necessary torsional stiffness, while concentrated longitudinal flanges or "spars" continued as before to take up the longitudinal stresses in bending. In the more modern airplane designs the shear stresses as well as the longitudinal stresses are taken up wholly or in part by a strong or sufficiently stiffened skin. In the following, this is considered as being typical of a "shell." In accord with this, a stiffened "shell wing" (fig. 1, right-hand side) has a large number of circumferentially distributed longitudinal flanges of approximately equal thickness supported by suitably close-spaced transverse flanges. The opposite transverse flanges of the upper and lower surfaces of the wing may be supplemented by webs or members to form

*"Zur Festigkeit von Schalen- und Rohrholmflügeln." From Luftfahrtforschung, vol. 14, nos. 4/5, April 20, 1937, pp. 179-190.

plate or truss ribs or else to form bending-resistant rings. Likewise, opposite longitudinal flanges can be joined to webs or members. A special case of this somewhat generalized concept of shell wing is the "pure shell wing," which has neither webs nor members (fig. 1, IIA).

In contrast with the "shell wing" (fig. 1, right-hand side), the spar wing (fig. 1, left-hand side) has only a few longitudinal flanges forming solid or trussed girders with webs or struts. For the diffusion of the shear stresses under torsion and in bending under transverse load in the plane of the wing, the skin of the spar wing may be utilized in various ways: On monospar wings (fig. 1, Ib), the nose itself usually serves for this purpose, supplemented at times by a central portion of the skin up to an auxiliary web. On two-spar wings (fig. 1, Ic), the skin between the spars is either utilized alone or in conjunction with the nose covering. The same holds for multispar wings (fig. 1, Id, Ie). The portions of the skin indicated by broken lines in figure 1 are usually not considered for the transmission of shear, those traced in thin outline are occasionally. A "pure spar wing" (fig. 1, Ia) is a wing whose spar, being of tubular design, is itself able to sustain the whole flexural and twisting stress of the wing and is stiff in twisting without participation of the skin. The different spar wings and the corresponding shell wings with and without webs are shown side by side in figure 1. The longitudinal stiffening of shell wings can be achieved by individual stiffener sections, corrugated sheet, or by flanging the webs or the skin. Joining the longitudinal stiffeners to the webs changes a shell wing to a spar wing, while the elimination of webs transforms a multispar wing into a shell wing.

While the shell-design method has found widespread use on bodies of modern metal airplane, the number of shell wings, particularly in Germany, is not very large. And this seems so much more surprising since the first metal wing ever built was a shell wing (fig. 2). This is the steel wing of the Junkers all-metal airplane built at the beginning of the World War. The longitudinal stiffness of the wing consists of corrugated sheet joined to the smooth skin; contrary to later Junkers practice, the corrugations run lengthwise with the wing. The suitability of this design was thus recognized by Junkers more than 20 years ago. The sketches in figure 1 represent shell wing types of leading airplane firms in the United States, where this design has found considerable favor. A particularly inter-

esting version is that of the three-web shell wing of the Douglas DC-2 (fig. 3). The continuous stiffeners form Z-sections on the upper surface and bulb angle sections on the lower. The ribs are solid walls with lightening holes and reach only to the inside edge of the stiffener sections to which they are attached by small angles. The lower part of figure 3 shows the riveted angle fitting of the outer panel bolted on the bottom side to the center section. Very few bolts are provided on the upper side; the compressive loads are transmitted through contact of the Z-sections widened out by corrugated straps and the circumferential angle. A recently designed single-web shell wing of the Henschel Company is shown in figure 4. The closely spaced longitudinal stiffeners of this wing consist of high hat sections with corrugated web. The solid ribs with flanged lightening holes extend as far as the skin and are perforated to pass the continuous longitudinal stiffeners. The outer wing panel is attached to the center section by a heavy extruded section, which transmits the compression through contact and the tension through bolts. We shall pass over the well-known German spar wings (fig. 1), but point to a new departure in spar design developed by the Hamburg Airplane Company. The wing has a tubular spar, which takes up all stresses and around which the other parts have been built. Figure 5 shows the junction point of the outer wing panel of a small airplane. The tubular spar of duralumin consists of two half shells riveted together top and bottom by one strap each. The outer spar fastens to the inner spar by means of the flange visible in figure 5, which in turn bolts onto the corresponding flange of the inner spar. Figure 6 shows the center section of a large airplane whose tubular spar of steel serves at the same time as fuel tank. The two halves of the steel spar are welded together. The light truss ribs to which the thin skin is riveted run with their flanges beyond the tubular spar to which they are attached by angle fittings.

2. Advantages and Disadvantages of

Spar-and-Shell-Type Wings

The real reason the shell wing has not found as much favor as the shell body is probably chiefly due to its constructional difficulties and higher cost of manufacture. If the airplane is large, the shell wing must be made in several parts, which implies strong and close-fitting joints. To avoid such a joint on the fuselage, the shell wing may

be made to pass through the fuselage if of the low-wing type. But then part of the otherwise available useful space is lost. On the spar wing, on the other hand, the design of the attachment fittings is substantially easier and, under otherwise identical conditions, obtainable with less weight than on the shell wing. Recesses for retractable landing gear, fuel tank, engine mount, and inspection panels on shell wings must be carefully faired in or covered in order to assure unobjectionable transmission of forces. The extensive division of the cross section makes a greater amount of supporting rivets necessary and renders the wing assembly difficult. These difficulties are less in the design and assembly of spar wings, especially with a tubular spar carrying all stresses, which also affords better facilities for servicing and repair.

From the point of view of strength, on the other hand, the advantages are more on the side of the shell wing. For bending stresses particularly the participation of the entire section lying in the outside region is propitious. Admittedly, it is to be observed that as a result of the extensive division of the supporting cross section of the shell wing, the crinkling and crippling strength in the compression zone is lower than on the spar wing where the concentrated compression flanges can frequently be utilized up to close to their material strength. But the thus obtained weight saving is generally less than the weight increase through the supplementary structural parts of the spar wing, that is, particularly through the skin, which in bending is not utilized to take up loads, but which for other reasons, such as good workmanship, strength in handling, or avoidance of severe wrinkling, for example, must be designed with a certain minimum weight.

The question of whether the skin is to be of the necessary minimum thickness or heavier, plays an important part on the shell wing. Under a uniform compression stress, the greatest load capacity is attained when the skin is as thin as possible and all other weight is carried in the stiffeners (reference 1). The latter, to insure high crinkling or crippling strength, are then spaced as far apart as consistent with the condition of no premature crinkling of the skin under service conditions. Then, however, the effect of cross-section distribution on the carrying capacity drops for heavier panels stressed under compression as represented by higher loaded shell wings. Besides, the transverse load on the shell wing carries, in contrast to the shell body, a substantial shear stress in the zone

of the high compressive stress. Then, if the skin is thin, it results in tension fields and consequently in additional compressive stresses which may neutralize the advantage of the higher buckling strength of the stiffeners (reference 2). Lastly, it should be remembered that with a thin skin, especially after the formation of tension fields, the shear stiffness of the panels also drops considerably and so causes, near cut-away sections, load application points, and junctions a more non-uniform distribution of the longitudinal stresses than with a thicker skin. For that reason, the shell wing with thin skin and heavy stiffener sections may, in contrast with the shell body, particularly with stronger cross section and greater transverse load, frequently afford no gain in carrying capacity. In such cases, it is then necessary to use a thicker skin and lighter stiffeners in order to utilize the advantages of the thicker skin with a view to better workmanship and smoother surface. Added to that, it affords, incidentally, greater stiffness and strength in torsion than for the shell wing with thin skin, since the sections of individual stiffeners by unrestrained warping contribute neither to the support of the twisting stress nor to the increase in twisting stiffness. The advantage of greater compressive strength with thin skin and heavier stringers without substantial decrease of strength and stiffness in shear is obtainable by stiffening the shell wing longitudinally with corrugated sheet. The suitability of corrugated sheet for shell-wing stiffening is discussed later on.

As regards strength and stiffness in torsion, the spar wing does not compare as unfavorably with the shell wing as for bending strength and bending stiffness. As extreme cases, we shall compare the tubular spar wing and the shell wing with optimum torsional stiffness. The latter is obtained with a conventional airfoil section by distributing the given weight over a shell which follows the wing contour up to two-thirds of the chord and terminates at a web separating the rear end of the wing (reference 3). If the weight of the tubular spar is placed around the shell as skin with uniform thickness, the torsional stiffnesses $(GJ_T)_S$ of the shell and $(GJ_T)_R$ of the tubular spar are in the ratio of

$$\frac{(G J_T)_S}{(G J_T)_R} = \left(\frac{F_S / F_R}{U_S / U_R} \right)^2$$

where F is the enclosed area and U the respective perimeter of the shell and the tubular spar.

The evaluation for a conventional airfoil section and a tubular-spar diameter of about 15 percent of the chord accordingly gives for the shell wing a torsional stiffness twice or three times as high as for the tubular-spar wing of identical weight, depending upon whether the torsional stiffness of the skin tube necessary on the tubular-spar wing is considered effective or not. (In the weight of the tubular-spar wing, this skin tube was figured as being about one-tenth of the wall thickness of the tubular spar.)

Now, however, in order to insure a compression-resistant cross section, part of the embracing tubular-spar weight must provide for the longitudinal stiffeners in the shell wing, which do not contribute to the torsional stiffness. It is only when the weight remaining for the skin amounts to more than one-third to one-half of the total weight, i. e., a fairly thick-walled shell wing, that the torsional stiffness of the shell wing is greater than that of the tubular spar type. On the shell wing stiffened with corrugated sheet, even a minor weight portion of the smooth sheet causes the torsional stiffness of the tubular-spar wing to be exceeded. These statements are valid to the extent that the torsional stiffness of the tubular spar wing or the shell wing does not decrease under increasing load (through exceeding the proportional limit or the buckling limit of the skin, for example). The above comparison refers, moreover, only to the torsional stiffness of the actual tubular spar and does not allow for the fact that on the tubular spar wing a rotation of the skin tube joined elastically by the ribs around the tubular spar itself may occur.

The ratio between the shear stress of the shell wing under torsion before buckling and the tubular spar wing of identical weight under elastic stress and the same assumptions as before, is:

$$\tau_S / \tau_R = \frac{E_R U_S}{E_S U_R} = \text{approximately } \frac{2}{3}$$

if the total tubular-spar section is placed around the shell skin. Accordingly, the torsional stiffness of a shell wing stiffened by individual sections and of the tubular-spar wing is the same if two-thirds of the total section is in the skin.

The statements regarding the advantages and disadvantages of spar-and-shell design of metal wings may be summed up as follows: A shell wing of equal flexural stiffness and not interrupted by cut-away sections and joints can, as a rule, be built lighter than a corresponding spar wing. With not too thin a skin or with corrugated sheet stiffening, such a shell wing then will have a torsional stiffness not inferior to that of a spar wing. However, the constructor must bear in mind that the design of joints and the deflection of the loads at cut-aways in a shell wing involve greater weight than on the spar wing, and that this weight increase may, under certain circumstances, balance the weight gain in the undisturbed zone of the shell wing.

II. STRESS CONDITION IN SHELL WINGS

1. Elementary Stress Condition under Bending and Torsion

The stresses in thin-walled, unstiffened or stiffened cylinders without intermediate longitudinal walls, as represented by shell bodies, has been treated in an earlier report (reference 1).

As concerns shell wings, the investigations need to be supplemented, since they are usually designed with intermediate longitudinal webs. If the shell section has several webs (fig. 7), the flexural stresses can be computed at once with the elementary flexure theory. Hereby, it is not necessary to refer the calculation to the principal axes of inertia. This means a simplified calculation of the shell wing, where, as a rule, no axes of symmetry exist.

Given the surface moments

$$J_z = \int_F y^2 s \, du, \quad J_y = \int_F z^2 s \, du, \quad J_{yz} = \int_F y z s \, du$$

as well as the respective bending moments B_z and B_y and the transverse loads Q_y and Q_z for any system of axes through the center of gravity S , the bending stresses are:

$$\sigma_x = \frac{\bar{B}_z}{J_z} y + \frac{\bar{B}_y}{J_y} z$$

with

$$\bar{B}_z = \frac{B_z - \frac{J_{yz}}{J_y} B_y}{1 - \frac{J_{yz}^2}{J_y J_z}} \quad \text{and} \quad \bar{B}_y = \frac{B_y - \frac{J_{yz}}{J_z} B_z}{1 - \frac{J_{yz}^2}{J_y J_z}}$$

The calculation of shear flow from the formula valid for any system of axes through the center of gravity

$$t = \tau \times s = \frac{\bar{Q}_y}{J_z} \underline{S}_z + \frac{\bar{Q}_z}{J_y} \underline{S}_y$$

with

$$\bar{Q}_y = \frac{Q_y - \frac{J_{yz}}{J_y} Q_z}{1 - \frac{J_{yz}^2}{J_y J_z}} \quad \text{and} \quad \bar{Q}_z = \frac{Q_z - \frac{J_{yz}}{J_z} Q_y}{1 - \frac{J_{yz}^2}{J_y J_z}}$$

is not at once possible except with an open or symmetrical closed section without webs or with center web, for which the zero places of the shear flow on the free sides or in the intersections of the axes of symmetry, needed for computing the static moments

$$\underline{S}_z = \int y s \, du \quad \text{and} \quad \underline{S}_y = \int z s \, du$$

are directly given.

To compute the shear flow for bending under transverse load in an unsymmetrical closed cross section or in a cross section divided by intermediate webs into n-part tubes (fig. 7) a single, or n times statically indeterminate calculation is necessary.* Cutting the n-part tubes on the circumference or on the webs in such a manner that a continuous shear flow becomes impossible in any part-tube, the cross section becomes an open cross section whose shear flow t_0 ,

*See also: Goodey, Shear Stresses in Hollow Sections, Aircraft Engg., vol. 8, 1936, pp. 93 to 95 and 102, where this calculation is made in a more roundabout way on the principle of minimum strain energy.

because of the then just sufficient zero places, can be determined from the above formula.

For the determination of the additive constant shear flows $\Delta t_1, \Delta t_2 \dots \Delta t_i \dots \Delta t_n$ possible on closed part-tubes, there are available the elasticity conditions that the torsion angles $\varphi_1, \varphi_2 \dots \varphi_i \dots \varphi_n$ of the n part-tubes referred to unit length shall, under torsion-free bending and by preservation of the cross-sectional form, become individually zero. For the i^{th} part-tube with the inclosed area F_i , we then obtain for a fictitious torque $\bar{T}_i = 2 F_i$, which produces in the part-tube the shear flow $|\bar{t}_i| = 1$:

$$\bar{T}_i \varphi_i = 2 F_i \varphi_i = \oint_i \bar{t}_i t_i \frac{du}{sG} = 0$$

The final shear flow t_i in the i^{th} part-tube is composed of the shear flow t_0 of the opened section ("statically determinate principal system") and the statically indeterminate constant shear flows $\Delta t_i, \Delta t_{i-1}$ and Δt_{i+1} in the part-tube (i) and in the adjacent part-tubes ($i-1$) ($i+1$). With the prefixes of figure 7, it is in the outer wall

$$t_{i,i} = t_0 + \Delta t_i$$

and in the left and right inside web

$$t_{i,i-1} = t_0 + \Delta t_i - \Delta t_{i-1}$$

and

$$t_{i,i+1} = t_0 - \Delta t_i + \Delta t_{i+1}$$

So, when observing that the fictitious shear flow in the outside wall (i,i) and in the left inside web is ($i, i-1$): $\bar{t}_i = +1$, but ($i, i+1$): $\bar{t}_i = -1$ in the right inside web, we have

$$\oint_i \bar{t}_i t_i \frac{du}{sG} = \oint_i t_0 \frac{du}{sG} + \Delta t_i \oint_i \frac{du}{sG}$$

$$- \Delta t_{i-1} \int_{i,i-1} \frac{du}{sG} - \Delta t_{i+1} \int_{i,i+1} \frac{du}{sG} = 0$$

With the abbreviations,

$$\varphi_{i,i} = \oint_i \frac{du}{sG}, \quad \varphi_{i,i-1} = \int_{i,i-1} \frac{du}{sG}, \quad \varphi_{i,i+1} = \int_{i,i+1} \frac{du}{sG}$$

$$\varphi_{i,o} = \oint_i t_o \frac{du}{sG} = \int_{i,i-1} t_o \frac{du}{sG} + \int_{i,i} t_o \frac{du}{sG} - \int_{i,i+1} t_o \frac{du}{sG}$$

it gives for the unknown shear flow Δt a system of three-term equations:

$$\begin{array}{r} \varphi_{1,1} \Delta t_1 - \varphi_{1,2} \Delta t_2 \qquad \qquad \qquad = - \varphi_{1,o} \\ - \varphi_{1,2} \Delta t_1 + \varphi_{2,2} \Delta t_2 - \varphi_{2,3} \Delta t_3 \qquad \qquad \qquad = - \varphi_{2,o} \\ \text{-----} \\ - \varphi_{i,i-1} \Delta t_{i-1} + \varphi_{i,i} \Delta t_i - \varphi_{i,i+1} \Delta t_{i+1} = - \varphi_{i,o} \\ \text{-----} \\ \qquad \qquad \qquad - \varphi_{n-1,n} \Delta t_{n-1} + \varphi_{n,n} \Delta t_n = - \varphi_{n,o} \end{array}$$

The solutions may be written in the form:

$$\Delta t_i = - \frac{\sum_{r=1}^n \alpha_{i,r} \varphi_{r,o}}{N} = - \frac{\alpha_{i,1} \varphi_{1,o} + \alpha_{i,2} \varphi_{2,o} + \dots + \alpha_{i,n} \varphi_{n,o}}{N}$$

where $\alpha_{i,k}$ and N denote functions of the values $\varphi_{i,k}$.

To illustrate: for $n = 1$ (no intermediate web)
and $n = 2$ (one intermediate web)*

$$\begin{array}{l} \alpha_{1,1} = 1 \qquad \qquad \qquad N = \varphi_{1,1} \\ \text{and} \\ \alpha_{1,1} = \varphi_{2,2}, \quad \alpha_{1,2} = \alpha_{2,1} = \varphi_{1,2}, \quad \alpha_{2,2} = \varphi_{1,1} \\ N = \varphi_{1,1} \varphi_{2,2} - \varphi_{1,2}^2 \end{array}$$

*The values α and N for other cases may be found in the work sheets of the DVL stress specifications, which also contain the determination of the shear center of thin-walled sections.

To insure torsion-free bending, the transverse loads Q_y and Q_z must be applied at the shear center M (fig. 7). If t_y denotes the shear flow due to $Q_y = 1$ and t_z due to $Q_z = 1$, the location of the shear center with respect to any axial system \bar{y}, \bar{z} parallel to axes system y, z through the center of gravity S follows from the condition that the torque of the transverse force is equal to the torque of the total shear flow acting in the material section F. (Torque, positive clockwise, transverse load, positive in negative y - z direction, fig. 7):

$$Q_y \times \bar{z}_M = Q_y \int_F t_y \times 2 d\bar{F}$$

$$Q_z \times \bar{y}_M = -Q_z \int_F t_z \times 2 d\bar{F}$$

From the previous derivatives then follow

$$\bar{z}_M = +2 \int_F t_y d\bar{F} = +2 \int_F t_{y,0} d\bar{F} + \sum_{i=1}^n 2 \bar{F}_i \Delta t_{y,i} = \bar{z}_{M,0} + \Delta \bar{z}_M$$

$$\bar{y}_M = -2 \int_F t_z d\bar{F} = -2 \int_F t_{z,0} d\bar{F} - \sum_{i=1}^n 2 \bar{F}_i \Delta t_{z,i} = \bar{y}_{M,0} + \Delta \bar{y}_M$$

with

$$t_{y,0} = \frac{J_y \underline{S}_z - J_{yz} \underline{S}_y}{J_y J_z - J_{yz}^2},$$

$$t_{z,0} = \frac{J_z \underline{S}_y - J_{yz} \underline{S}_z}{J_y J_z - J_{yz}^2}$$

$$\Delta t_{y,i} = - \sum_{r=1}^n \frac{\alpha_{i,r}}{N} \oint_r t_{y,0} \frac{du}{sG}, \quad \Delta t_{z,i} = - \sum_{r=1}^n \frac{\alpha_{i,r}}{N} \oint_r t_{z,0} \frac{du}{sG}$$

$$\underline{S}_y = \int_0 u z s du,$$

$$\underline{S}_z = \int_0 u y s du$$

Herein $\bar{z}_{M,0}, \bar{y}_{M,0}$ denote the distances of the shear center for the opened-up section in the \bar{y} and \bar{z} system of axes and $\Delta \bar{z}_M, \Delta \bar{y}_M$, the distances of the shear center of the opened-up and closed section from one another.

If the external forces in the cross-sectional plane are applied outside the shear center, their effect may be replaced by transverse loads Q_y, Q_z in the shear center and a pure twisting moment T about the longitudinal axis. Then the shear flow due to T can be obtained in the same

manner as the shear flow due to transverse load. In this case, the condition is that all part-tubes must twist through the same angle φ (reference 4):

$$\varphi_1 = \varphi_2 \dots = \varphi$$

Then the energy equation gives for the i^{th} part-tube with the enclosed section \underline{F}_i :

$$\overline{T}_i \varphi_i = 2 \underline{F}_i \varphi_i = \oint_i \overline{t}_i t_i \frac{du}{sG} = 2 \underline{F}_i \varphi$$

Since $t_0 = 0$, hence $t_i = \Delta t_i$ under pure twist, it again affords a system of three-term equations for the unknown shear flows t_i in the part-tubes where the left-hand side agrees with the equations for transverse load, whose load terms in the present case are:

$$\varphi_{i,0} = -2 \underline{F}_i \varphi$$

The solutions then assume the form:

$$t_i = 2 \sum_{r=1}^n \alpha_{i,r} \underline{F}_r \frac{\varphi}{N} = 2 A_i \frac{\varphi}{N} \quad \text{with} \quad A_i = \sum_{r=1}^n \alpha_{i,r} \underline{F}_r$$

The still unknown angle of twist φ follows from the condition that the sum of all partial moments T_i must give the total twisting moment T :

$$\sum_{i=1}^n T_i = \sum_{i=1}^n 2 \underline{F}_i \times t_i = 4 \frac{\varphi}{N} \sum_{i=1}^n A_i \underline{F}_i = T$$

whence

$$\frac{\varphi}{N} = \frac{T}{4 \sum_{i=1}^n A_i \underline{F}_i}$$

and the shear flows in the part-tubes are:

$$t_i = \frac{A_i}{2 \sum_{i=1}^n A_i \underline{F}_i} T$$

which gives, on the circumference: $t_{i,i} = t_i$ and on the right- and left-hand intermediate web:

$$t_{i,i-1} = t_i - t_{i-1} \quad \text{and} \quad t_{i,i+1} = t_{i+1} - t_i$$

The torsional stiffness of a multiweb shell section is given with:

$$G J_T = \frac{T}{\varphi} = \frac{4}{N} \sum_{i=1}^n A_i \underline{F}_i$$

The values $\alpha_{i,k}$ for computing A_i and N are again the same functions of the values $\varphi_{i,k}$ as under transverse load and may be obtained for other numbers of intermediate webs from the cited work sheets. For the simplest case $n = 1$ (no intermediate web) equation

$$\alpha_{1,1} = 1, \quad A_1 = \underline{F}_1 \quad \text{and} \quad N = \varphi_{1,1} = \oint \frac{du}{sG}$$

gives the known Bredt formulas:

$$t_1 = \frac{T}{2 \underline{F}_1}, \quad G J_T = \frac{4 \underline{F}_1^2}{\oint \frac{du}{sG}}$$

The determination of the shear flow in multiweb stiffened sections must be effected with a different effective shear stiffness of the shell surface depending upon the type of stiffener and condition of the skin. In the case of individual stiffeners and buckling-resistant skin, we must count with the shear stiffness sG (s = skin thickness, G = shear modulus) as on the unstiffened shell; for corrugated sheet stiffeners of wall thickness s_w , spacing b and arc length b_w the effective shear stiffness is $(s + s_w b/b_w)G$.

On stiffened shells with skin panels buckled under shear, the shear stiffness drops as the excess of critical shear stress τ_k increases. Then a reduced shear modulus

depending on the load replaces $G = \frac{E}{2(1 + \nu)}$.

According to experiments by Lahde and Wagner (reference

5), the drop for flat sheet panels is approximately linear with $\sqrt{\tau_k/\tau}$ from value G of the shear-resistant panel to the value G' of the uniaxial tension field. The reduced shear modulus follows according to the tension-field theory (reference 6) from the displacement of the homogeneous strain field and amounts, on the uniaxial tension field, to

$$G' = \frac{\tau}{\gamma} = \frac{E}{2(2 - \sigma_x/\sigma - \sigma_y/\sigma)}$$

Here σ , σ_x , and σ_y , respectively, denote the principal tensile stress and the stress of the side members. In the specific case of rigid side members ($\sigma_x = \sigma_y = 0$),

$G' = \frac{E}{4}$; under great compressive stress compared to shear stress (σ_x/τ or $\sigma_y/\tau \rightarrow -\infty$) $\frac{G'}{E}$ gradually goes to zero.

Since, for stiffened shells with buckled sheet panels, the relevant shear stiffness depends upon the size of the load, the statically indeterminate calculation is restricted to a particular loading condition, such as failing load, for example. The final stress condition resulting from this load must be estimated for the calculation; if the estimate is off the calculation can be improved progressively. In the determination of the reduced shear modulus, the usually unlike stresses in the side members of the tension fields are expressed by mean values.

On curved buckled sheet panels, the smooth pulling of the curved skin and radial resilience of the stiffeners are also of influence on the shear strain (reference 7). Additional details on the stress condition of stiffened shells with buckled flat or curved sheet panels will be found in the writer's report on the strength of shell bodies (reference 1).

2. Secondary Stress Condition Due to Applied Load

And Restrained Cross-Sectional Warping

The validity of the investigations so far was based on the assumptions of elementary beam theory, e.g., for an applied load conformably to the elementary stress distribution, as well as for bending under transverse load and

twisting with unrestrained warping. If these assumptions are not satisfied, secondary internal stress conditions occur which superpose themselves on the elementary stress conditions.

The magnitude of secondary stresses at the point of load application is defined by the difference of the initiated stresses from those of the elementary theory; at the points of restrained warping, it is governed by the difference of the unrestrained warping in adjacent sections. Warping in bending under transverse load or twist occurs when the shell departs from the circular form or when its shear stiffness varies over the circumference. The differences in such warping are so much greater as the transverse forces, respectively, the twisting moments or else the dimensions in the adjacent sections are different. The secondary stresses necessary to balance the warping discrepancies become so much higher as the shear stiffness, compared to the longitudinal stiffness, is lower. The assumptions for higher secondary stresses due to restrained warping are accordingly given in greater measure on the shell wing than on the shell body.

The disappearance of the secondary stresses due to applied load (reference 8) or to restrained warping is governed by their circumferential distribution and the stiffness of the system. Great stiffness of the longitudinal flanges relative to the shear stiffness of the skin and inside webs or in relation to the transverse stiffness of the system afforded by the ribs or bulkheads, invariably leads to a slow - in the extreme case, linear - disappearance of the secondary stresses. Great transverse stiffness of shell, as, for instance, on a shell wing with solid or truss ribs causes a quick disappearance even by internal stress conditions which first come in equilibrium in a more curved or polygonal circumferential zone of the shell. The disappearance of such "spatial internal stress conditions" - as, for instance, in torsion with restrained warping and under axial load application - is so much quicker by great transverse stiffness of the shell as the shear stiffness of the longitudinal walls is greater; absence of spatial transverse stiffness of the system on the other hand, even by great shear stiffness of the longitudinal walls, renders the disappearance of these internal stresses gradual.* For the disappearance of the "plane internal

*For the determination of such stresses in stiffened and unstiffened shells, see Luftfahrtforschung, vol. 14, 1937, no. 3, p. 96, part II, 2 and 3, as well as the references quoted.

stress conditions" extending to smaller and particularly to flat or slightly curved areas, on the other hand, the plane transverse stiffness of the skin acting then as "disk" or of the longitudinal webs is decisive. If this is sufficiently great, the disappearance by great shear stiffness compared to longitudinal stiffness is rapid and, by low shear stiffness gradual.

The flat or slightly curved top and bottom sides of a shell wing then resemble stiffened plates with rib flanges furnishing sufficient transverse stiffness. So, while the shear stiffness of the bottom side stressed in tension in the decisive load cases remains unchanged under load, that of the compressed upper side decreases, especially on thin-walled stiffened shells after exceeding the buckling load in the sheet panels because of the formation of tension fields (c.f. II, 1). For this reason, the compression zone of shell wings involves greater and slower disappearing secondary stresses. This indicates that in bending, especially in the vicinity of the load application and restrained warping*, as, for instance, at junctions and cut-away sections of a shell wing, a weaker cooperation of the central area of the compression zone takes place.

The stress condition of axially loaded side members of stiffened plates has been explored both theoretically and experimentally (ref. 9 and 10). The experimental results are in good agreement with theoretical values established on the assumption of constant stringer spacing, i.e., great transverse stiffness of the plate. For clarification of the stress condition in stiffened shell wings under transverse loads, some experiments were made by the DVL. The experimental wing (fig. 8) represents the center section of a two-web shell wing. The stress distribution in the compression zone being the center of interest, the wing was first designed as an open trough and the omitted tension zone replaced by strong tension flanges on the lateral webs.

This arrangement favored the testing procedure to the extent of making every part of the wing accessible for strain measurements. The compression zone was a slightly curved 1.2-millimeter-thick duralumin skin over closed

*The case of restrained warping of the wide, unstiffened, flange plates of a box section in bending under transverse load has been treated by von Schnadel, Werft Reed. Hafen Bd. 9, Nr. 5, 1928, and under flexural twist by the author in Z.f.a.M.M., Bd. 14, Heft 6, 1934.

hat-section stiffeners; the edge stiffeners on the webs were thick angle sections. The upper, four-cornered duralumin tension straps were bolted to the edge angles, so that they could be removed and the test specimen be converted into a closed box girder through a continuous tension zone and so be used for torsion experiments. An intermediate web may be inserted, if desired, between the divided ribs and the two separate sections of the middle stringer. The truss ribs with hat-section flanges and C-section lattices are spaced 50 centimeters apart over the continuous stringers.

The set-up for bending is shown in figure 9. The compression zone of the test piece is bolted to a heavy steel plate of the frame by means of an angle. The tension strap passes through this and joins on a box girder between the frame supports. Wedges between the stiffener face and the steel plate provide for the transfer of the stringer compression forces. The frame being hinged at all four corners permits the application of pure bending moments, on special lugs transverse loads at the end and on the intermediate ribs to the webs. The loads are applied by hand cranks.

The first experiments on the described test specimen were transverse loads applied at the end prior to buckling of the skin. The strains were measured on all stringers between the ribs (see fig. 10) under concentrated loads $P = 765 \text{ kg}$ on every web. The mean values of the longitudinal stresses σ_x evaluated with an elasticity modulus of $E = 740,000 \text{ kg/cm}^2$ are shown in figure 10 as ordinates against the test points and combined to a stress concentration by heavy lines. The longitudinal stresses computed according to the elementary bending theory and shown as thin lines, are greater in the center of the sections than at the edges, on account of the curved compression zone. The comparison between the measured and the computed stresses discloses in the central sections a good agreement between elementary theory and test, whereas near the point of fixation the anticipated disturbances of the elementary stress condition can be observed. The introduction of the transverse loads $2P$ does not agree with the shear flow distribution t_0 postulated by the elementary theory but rather denotes - disregarding the minor disturbance at the webs - the introduction of a secondary shear flow Δt in the compressive zone (fig. 10, left-hand side). In this particular test, the stiff edge angle at the load section had been removed which shifted the equalization of this

secondary load over to the adjoining shell. A second test with angles attached disclosed no disturbance of the elementary stress condition under transverse load. The secondary stresses at the point of fixity are due to the restrained warping in the shell area. With unrestrained warping, it would assume the shape of the line shown on the right-hand side of figure 10. The equalization of the warping difference between shell and frame then requires the illustrated secondary stresses as they were actually observed in the test. Additional strain measurements under other loads as well as after buckling of the sheet panels between the stiffeners are to be made.

III. FAILING STRENGTH OF SHELL WINGS

1. Failing Strength under Bending and Torsion

The load capacity of a stiffened shell wing with thick skin, which is buckling-resistant up to failure under bending or torsion, is given by the buckling strength of an orthotropic plate or shell (reference 11). The critical buckling stress $\sigma_{k,o}$ of an orthotropic shell stressed in compression only is afforded from Dschou's formulas (reference 12). The buckling strength of the orthotropic shell under combined compression and shear has not been investigated so far. But in most cases it will be possible to estimate the buckling strength of the slightly curved compression zone stressed in shear only from the buckling stress $\tau_{k,o}$ of the identically dimensioned and identically stressed orthotropic plate (reference 13), and to determine the correlated critical compressive and shearing stresses σ_k and τ_k under the combined effect of which the orthotropic plate or shell buckles, from the formula

$$\left(\frac{\tau_k}{\tau_{k,o}} \right)^n = 1 - \frac{\sigma_k}{\sigma_{k,o}} \quad (n = 2 \text{ to } 3)$$

The load capacity of a stiffened shell wing with sheet panels buckled prior to failure is primarily given by the buckling strength of the stringers elastically imbedded through the skin. Owing to the extremely complicated effects of the skin on the buckling process, it was advisable in the determination of the compressive strength of shell bodies to ascertain the compressive strength of

the compression zone by a compression test on a panel patterned after a full shell (reference 1, III, 1). With certain limitations, this method is applicable also to the determination of the failing strength of shell wings. In contrast to the minor shear forces in the zones of a shell body largely stressed in compression owing to bending, these zones in the shell wing also manifest considerable shearing stresses. So the panel test should preferably be made for combined compression and shear, which is, however, experimentally difficult.

But, as in the case of the shell body, the failing stress $\sigma_{L,B}$ of the stiffeners can also be ascertained from a compressive panel test by means of the effective width or else from stress measurements and these can be compared with the stiffener stresses computed for the shell wing with respect to the secondary stresses due to the tension fields, after which the cumulative stresses due to load application or restrained warping can be added. This method is an approximation insofar as the wrinkling of the skin in the wing shell under combined compression and shear is unlike that of the panel under pure compression. Since the bulging of the stringers by slightly different wall thicknesses of skin and stringer is induced by skin wrinkles and since any change in the wrinkling is thereby of some influence, according to Kromm's experiments (reference 14), the actual failing stress must be computed from the value obtained in the panel test. On the contrary, the elastic support of the skin effective for the lateral instability and torsional buckling of the stringers is not materially affected by a changed wrinkling formation.

The transverse loading of the shell wing due to distributed surface loading can, just as the radial secondary load due to deflection of the tension fields, be duplicated in the panel test. In this manner, the strength of the shell wing can be ascertained by panel test for torsion and combined bending and torsion (reference 1, III, 2).

2. Load Capacity of Curved Panels with Corrugated Sheet or Separate Stiffeners

The curved panel test can also be used for the determination of the best cross-section design by equal weight. And a large number of such tests have already been made for this purpose incidental to the investigations of shell

body strength. But, as the shells involved on shell wings have, as a rule, a stronger sectional covering of the circumference and less curvature than on shell bodies, the panel tests were supplemented by tests on flat stiffened panels of greater average skin thickness (c.f. table I).

The appraisal of the cross-section design of the shell wing must, apart from the compressive strength in the panel test, include at the same time the shear strength and shear stiffness existing in the explored cross-section design because of the decisive shear stress on the shell wing. But the very shell-section design of thin skin and strong individual sections, which favors the compressive strength, is associated with low shear stiffness and shear strength, hence, unfavorable for the shell wing stressed simultaneously in shear. This drawback of the thinner skin is, however, largely counteracted with stringers of corrugated sheet, which takes up part of the shear and so contributes to the shear strength and the shear stiffness. A further advantage of corrugated sheet stiffeners is the delayed buckling of the smooth sheet on account of the more narrow subdivision of the smooth skin and its lower shear stress. The result of the thus incompletely formed tension fields is a lower secondary stress in the longitudinal stiffeners (reference 15) and a smaller decrease in the shear stiffness of the smooth sheet under rising load. Besides, since the shear stiffness of the corrugated sheet remains unchanged up to failing load, the total shear stiffness of the shell with corrugated sheet decreases more slowly yet. Thus the shell wing stiffened with corrugated sheet insures through its greater and more uniform shear stiffness a more uniform stress distribution in bending and torsion, as well as lower secondary stresses due to force introduction and restrained warping adjacent to junctions and cut-away.

Prompted by the advantages cited of corrugated sheet stiffeners for shell wings, a number of tests were made with flat corrugated panels of varying circumferential shapes characterized by the mean wall thickness s_m (table I). The wave form and the thickness ratio of corrugated to smooth sheet was varied on the panels. The usual sinusoidal shape and another made up of two semicircles of different diameters were selected, the corrugated sheet being joined to the smooth sheet on the side of the smaller semicircles (table I). The corrugated shells were neatly matched and fitted at the ends with duralumin bands in imitation of the rib flanges (fig. 11). The failure of the panels with semicircular corrugations occurred in the

majority of cases through bulging of the wave lying against the smooth sheet despite its greater curvature (fig. 11). On the panels with sinusoidal corrugations, however, the bulging frequently started at the shoulders in the vicinity of a turning point of the curvature.

The results of the compression tests with corrugated panels are given in table I. Series 1 to 6 reveal the influence of the wave form on the load capacity for approximately equal average wall thickness s_m and for a corresponding distribution of section over corrugated and smooth sheet. According to this, the mean failing stress $\sigma_{m,B}$ serving as indication of the load capacity, on the shells stiffened with semicircular corrugations is only about 5 to 10 percent higher than on the shells with sinusoidal corrugations. The effect of a different section distribution on corrugated and smooth sheet is also shown. While the distribution in series 1 to 4 was so chosen that both types of sheets had approximately the same wall thickness, the smooth sheet of series 7 to 9 was thinner. As a result of this, the shells with thinner average wall thickness ($s_m = 1.7$ mm, series 2 and 7) had about 50 percent higher load capacity under compression, whereas the difference in load capacity of the thicker shells ($s_m = 2.2$ mm, series 4 and 8) amounts to only about 17 percent. It should be noted, however, that the shear stiffness of shells with thinner smooth sheet drops by about 15 percent.

The results of the compression tests on corrugated sheet shells and shells stiffened by separate sections are shown side by side in table I. With one exception, these shells were so designed that their shear stiffness was not substantially inferior to that of the shell of corrugated sheet. For comparison of the shear stiffnesses, the last column of the table gives the ratio of the reduced shear modulus referred to average wall thickness to the elastic

shear modulus: $\frac{G'}{G}$ (cf. II, 1).

Comparison of the mean failing stresses discloses the corrugated sheet shells (series 7 to 9, top) with on the average still somewhat higher shear stiffness to possess about 25 to 35 percent greater load capacity than the shells with individual stiffeners and corresponding mean wall thickness (series 1, 2, 4, and 5 bottom). Only one shell of the latter type in series 3 having a considerably lower shear stiffness approximately approaches the carrying capacity of the corrugated sheet shell (to within about 10 percent).

The table finally shows (see also fig. 12) the first somewhat faster - then on approaching the yield limit slower - rise in failing strength with increasing mean wall thickness. Figure 12 shows the failing stress of corrugated sheet plotted against wall thickness, for corrugated sheet alone and in combination with riveted smooth sheet of different thicknesses. The failing stress of the corrugated sheet in conjunction with thicker smooth sheet decreases in spite of the greater mean wall thickness. The reason for this is that the buckling is more intensely excited through the thicker smooth sheet.

IV. STRESS CONDITION AND FAILING STRENGTH OF TUBULAR SPARS

The previously cited advantages in the design and manufacture of tubular spar wings, in spite of the incomplete utilization of the tubular spar in bending, have led to its rapidly expanding use, especially as a result of the Hamburger airplane design. From the static point of view, the design has the advantage of very simple stress analysis as a result of the clear, static structure. Since the wing spar is designed to carry the total wing load by itself, the load grading for bending and torsion relative to shear center is directly possible. The stresses in the elastic range conform to the elementary bending and torsion theory. Disturbances in the stress conditions due to restrained warping are altogether absent because of the round form of the spar, the secondary stresses due to load application are lower, and the considerations concerning the changes in stress condition and stiffness after buckling are eliminated.

However, the advantages are contingent upon correct data about the obtainable strength in bending and tension. A theoretical analysis of this strength is difficult to achieve; on thin-walled tubes of large ratio d/s (d = diameter, s = wall thickness) which buckle in the elastic range, the manufacturing defects in the geometrical form have a marked effect on the strength. On thick-walled tubes which buckle in the super-elastic range, the material properties and their scatter play a prominent part. For these reasons, the making of systematic experiments is necessary. The bending and compression tests of Lundquist (reference 16) and of Donnell (reference 17) on duralumin and steel, from which some information about the expected bending strength is obtainable, cover only the elastic

range ($\frac{d}{s} > 300$ to 400). Among the bending and compression tests in the super-elastic range are those by Robertson (reference 18) on steel tubes with comparatively thick-walled tubes ($\frac{d}{s} = 20$ to 100) and more recently, the experiments by Stender.* Systematic bending and compression tests in the more important range ($\frac{d}{s} = 100$ to 300) other than isolated compression tests on special materials, are lacking. The same is true of tests in torsion and combined bending and torsion.

In order to fill this gap, the DVL in collaboration with the Hamburg airplane firm has launched an elaborate program of bending and compression tests on steel tubes of $\frac{d}{s} = 60$ to 270. To assure a maximum of uniform material strength all tubes had the same wall thickness $s = 1.5$ mm. This called for the design of a testing machine with an ultimate bending moment of around 12 mt. Figure 13 illustrates the mounting of a tube on the powerful frame. The flanges riveted to the tube are bolted to a thick steel plate reinforced by ribs, which, to accommodate tubes of different diameters, was fitted with numerous threaded holes. The load was applied at a correspondingly designed counterplate on which oppositely directed horizontal forces were applied above and below through a special loading device.

By means of suitable rotation of the loading device about the hinges with vertical axis on the counterplate, the tubes can be stressed in pure bending, in pure torsion, or in combined bending and torsion.

The test program was started with a portion of the bending tests and the corresponding compression tests. The failure of the tubes in bending is caused by the buckling of the compressive zone at stresses which for the explored $\frac{d}{s}$ (= 60 to 270) lie in the superelastic range. Tubes

*Unpublished report of the Hamburg airplane firm which also contains a list of practically every known experiment.

stressed in pure compression (figs. 14a and 14b) exhibit a very similar form of failure. It is therefore to be expected that the failing strength in bending is, exactly as in compression, largely dependent upon the wall ratio d/s but only little on the length ratio l/d as confirmed in preliminary tests.

The ultimate stress $\sigma_B = B_{Br}/W$ (B_{Br} = ultimate bending moment) as computed by elementary bending theory serves as indication for the bending resistance. For various reasons, this stress σ_B must be greater than the failing stress of the corresponding compression test $\sigma_D = P_{Br}/F$ (P_{Br} = compressive load at failure). Because in the compression test every point is subject to maximum stress, while in the bending test only the extreme compressive zone is subjected to the maximum stress, which creates a "supporting effect" of the incompletely stressed zones. This "supporting effect" exists in the elastic as in the superelastic range. Besides, a stress balance may take place in the outer zones, because in the present d/s range the outer fibers are stressed beyond elasticity, so that the stress σ_B computed by elementary bending theory merely indicates a fictitious - albeit too high - a value. Added to that, the defects in geometrical form and the scatter of material characteristics have a more unfavorable effect in the compression than in the bending test because of the smaller range of the adverse stress in the bending test.

The completed bending and compression tests confirm that the previously defined bending strength is higher than the compression strength, the ratio of bending to compression strength amounting to about 1.2 to 1.3 for the smaller $d/s = 60$ to 120. However, in order to adequately cover this ratio for greater d/s values also, a greater number of bending and compression tests is necessary, particularly since the latter is accompanied by unavoidable scattering.

Strain measurements were made at several points of the circumference of various tubes prior to failure (fig. 13). The stress condition resulting from these strains with a constant $E = 2.1 \times 10^6$ kg/cm² is shown in figure 15 for a tube of $d/s = 150$. The comparison of the measured stresses with those computed by elementary bending theory manifests a good agreement at the lower load stages.

At the highest load stage, which is about 80 percent of the failing load, the compression zone reveals a difference between measured and computed values. The plotted values beyond the proportional limit (3,000 to 4,000 kg/cm²) are fictitious. The strains measured after they exceeded this limit would have to be multiplied by a lower elastic modulus and, indeed, earlier in the compression than in the tension zone because of the Bauschinger effect. This explains the apparent excess stress in the compression zone. The non-linear strain distribution is attributable to the change in cross-sectional form during loading.

Translation by J. Vanier,
National Advisory Committee
for Aeronautics.

REFERENCES

1. Ebner, H.: The Strength of Shell Bodies - Theory and Practice. T.M. No. 838, N.A.C.A., 1937.
2. Sommer, A.: Beitrag zur Querschnittsbemessung des zweistegigen Schalenflügels. Dornier-Post, No. 9, Feb.-March, 1937.
3. Cox, Harold Roxbee: Stiffness of Thin Shells. Airc. Engg., vol. VIII, no. 91, Sept. 1936, pp. 245-246.
4. Lorenz, H.: Techn. Elastizitätslehre. Oldenbourg, München and Berlin, 1913, p. 105 ff.

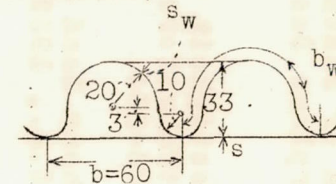
Hertel, H.: Verdrehsteifigkeit und Verdrehfestigkeit von Flugzeugbauteilen. Luftfahrtforschung, Bd. 9, Lfg. 1, Aug. 1, 1931, p. 24.
5. Lahde, R., and Wagner, Herbert: Tests for the Determination of the Stress Condition in Tension Fields. T.M. No. 809, N.A.C.A., 1936.
6. Wagner, Herbert: Flat Sheet Metal Girders with Very Thin Metal Web. T.M. Nos. 604, 605, and 606, N.A.C.A., 1931.
7. Wagner, Herbert, and Ballerstedt, W.: Tension Fields in Originally Curved, Thin Sheets during Shearing Stresses. T.M. No. 774, N.A.C.A., 1935.
8. Wagner, Herbert, and Simon, H.: Über die Krafteinleitung in versteiften Zylinderschalen. Luftfahrtforschung, Bd. 13, Lfg. 9, Sept. 20, 1936, pp. 293-308.
9. White, Roland James, and Antz, Hans M.: Tests on the Stress Distribution in Reinforced Panels. Jour. Aeron. Sci., vol. 3, no. 6, April 1936, pp. 209-212.
10. Lovett, B. B. C., and Rodee, W. F.: Transfer of Stress from Main Beams to Intermediate Stiffeners in Metal Sheet Covered Box Beams. Jour. Aeron. Sci., vol. 3, no. 12, 1936, pp. 426-430.

11. Heck, O. S., and Ebner, Hans: Methods and Formulas for Calculating the Strength of Plate and Shell Constructions as Used in Airplane Design. T.M. No. 785, N.A.C.A., 1936.
12. Dschou, Dji-Djüän: Die Druckfestigkeit versteifter zylindrischer Schalen. Luftfahrtforschung, Bd. 11, Lfg. 8, Feb. 6, 1935, pp. 223-234.
13. Seydel, Edgar: The Critical Shear Load of Rectangular Plates. T.M. No. 705, N.A.C.A., 1933.
14. Kromm, A.: Einfluss der Nietteilung auf die Druckfestigkeit versteifter Schalen aus Duralumin. Luftfahrtforschung, Bd. 14, Lfg. 3, March 20, 1937, pp. 116-120.
15. Schapitz, E.: Contributions to the Theory of Incomplete Tension Bay. T.M. No. 831, N.A.C.A., 1937.
16. Lundquist, Eugene E.: Strength Tests of Thin-Walled Duralumin Cylinders in Pure Bending. T.N. No. 479, N.A.C.A., 1933. Strength Tests of Thin-Walled Duralumin Cylinders in Compression. T.R. No. 473, N.A.C.A., 1933.
17. Donnell, L. H.: A New Theory for the Buckling of Thin Cylinders under Axial Compression and Bending. A.S.M.E. Trans., vol. 56, no. 11, Nov. 1934, pp. 795-806.
18. Robertson, Andrew: The Strength of Tubular Struts. R. & M. No. 1185, British A.R.C., 1937.

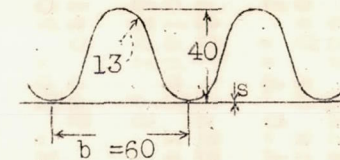
Table I - Compressive Strength and Shear Stiffness of Flat Sheets Stiffened with Corrugated Sheet
or with Separate Sections. (Length of panes $l = 500$ mm)

Corrugated sheet (see fig.)	Mean wall thickness s_m	Wall thickness of sheet		Buckling stress of smooth sheet σ_k	Failing stress of corrugated sheet $\sigma_{w, B}$	Mean failing stress $\sigma_{m, B}$	$\frac{G'}{G}$
		Smooth s	Corrugated s_w				
	mm	mm	mm	kg/cm ²	kg/cm ²	kg/cm ²	-
Sinusoidal	1.69	0.60	0.59	400	1800	1550	0.54
Half circle	1.58	.60	.60	430	1950	1650	.60
Sinusoidal	2.26	.83	.79	820	2300	2040	.54
Half circle	2.16	.80	.81	840	2600	2260	.60
Sinusoidal	3.70	1.50	1.19	1900	2500	2430	.57
Half circle	3.61	1.61	1.20	2200	2600	2520	.64
Half circle	1.75	.50	.81	520	3000	2470	.53
Half circle	2.24	.49	1.03	560	3100	2630	.50
Half circle	2.72	.74	1.20	670	3000	2550	.53

Corrugated sheet stiffener
Half circle:



Sinusoidal:



Mean wall thickness:

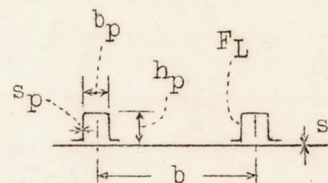
$$s_m = s + s_w \frac{b_w}{b}$$

Reduced shear modulus:

$$G' = G \frac{s + s_w \frac{b_w}{b}}{s + s_w \frac{b_w}{b}}$$

Channel form	Mean wall thickness	Thickness of skin	Division	Buckling stress of skin	Failing stress of stiffeners	Mean failing stress	$\frac{G'}{G}$
$\frac{h_p}{b_p} s_p$	s_m	s	b	σ_k	$\sigma_{L, B}$	$\sigma_{m, B}$	
- mm	mm	mm	mm	kg/cm ²	kg/cm ²	kg/cm ²	-
$\frac{30}{20}$ 1.5	1.82	0.82	140	700	2450	1950	0.45
$\frac{20}{18}$ 1.2	2.28	1.51	105	1700	2330	1930	.66
$\frac{33}{23}$ 1.5	2.20	.50	105	190	2750	2400	.22
$\frac{40}{30}$ 1.5	2.70	1.20	140	800	2200	1880	.44
$\frac{35}{25}$ 1.5	2.73	1.03	105	720	2400	2020	.38

Individual channel stiffeners



Mean wall thickness:

$$s_m = s + \frac{F_L}{b}$$

Reduced shear modulus:

$$G' = G \frac{s}{s_m}$$

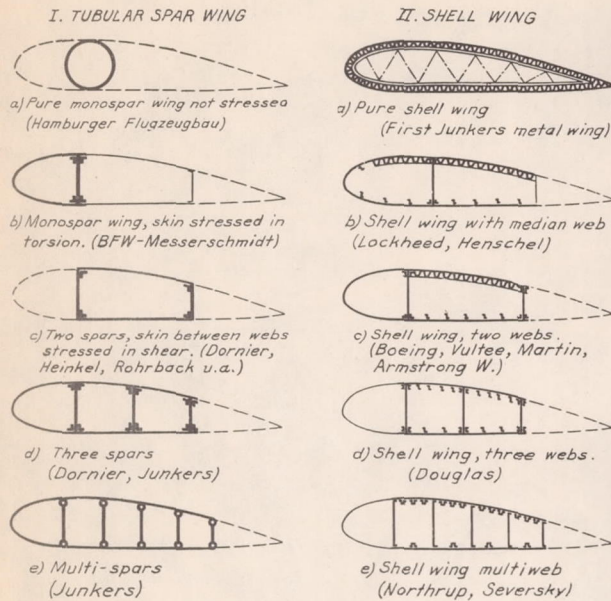


Figure 1.- Different versions of tubular spar and shell wings.

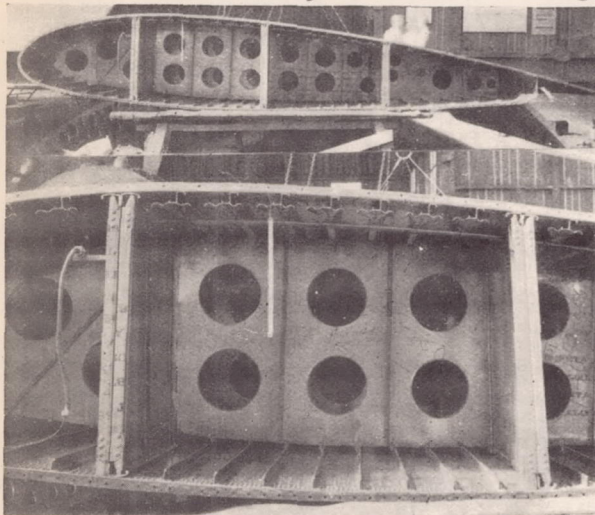


Figure 3.- Douglas DC-2, showing 3 webs.

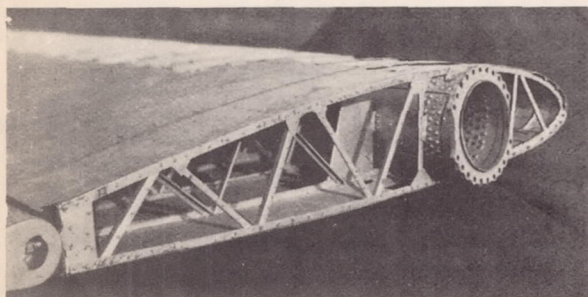
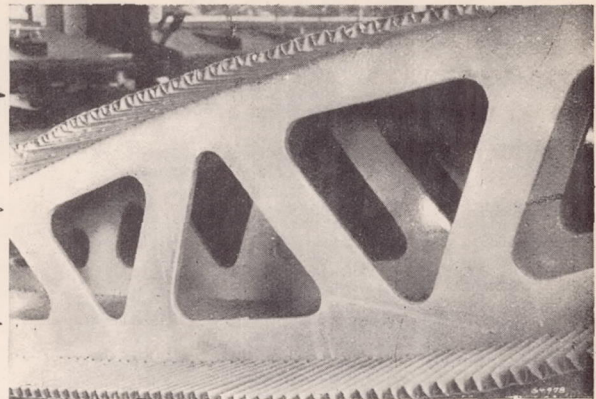
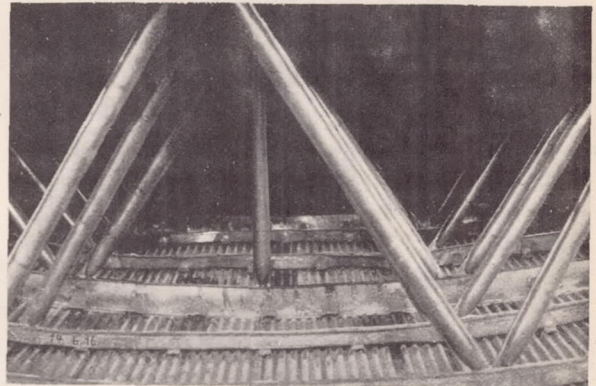


Figure 5.- Outer tubular spar-wing of Hamburger-Flugzeugbau.



2 a. Experimental design



2 b. Final design

Figure 2a & 2b.- Design of first Junkers all metal wing.

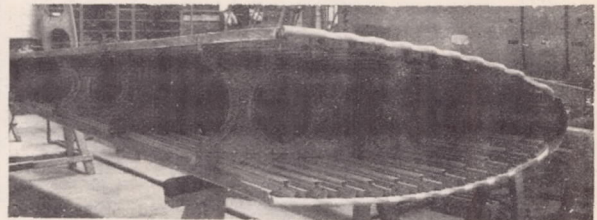


Figure 4.- Henschel single-web shell wing.

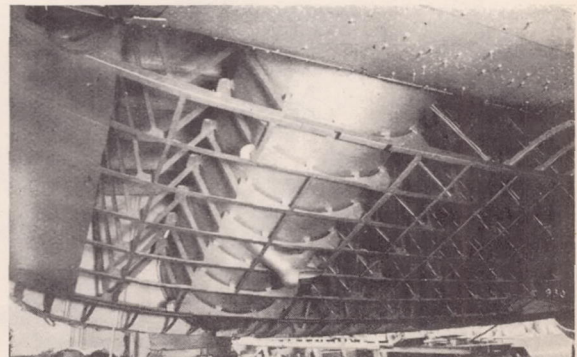


Figure 6.- Center section of large tubular spar wing of Hamburger-Flugzeugbau.

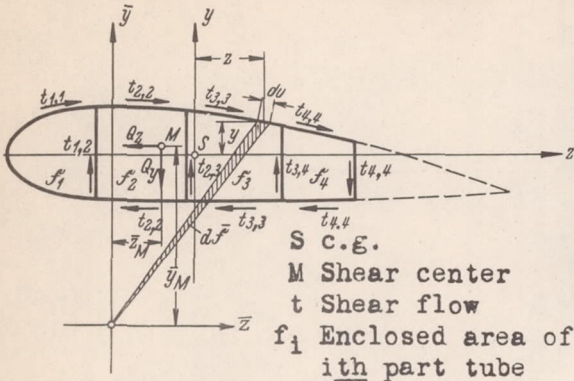


Figure 7.- Multi-web shell section - notation.

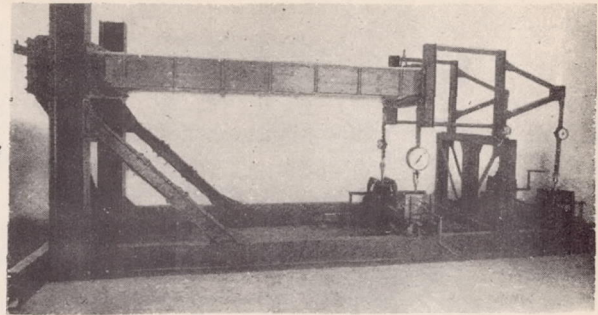


Figure 9.- Loading device with experimental wing.

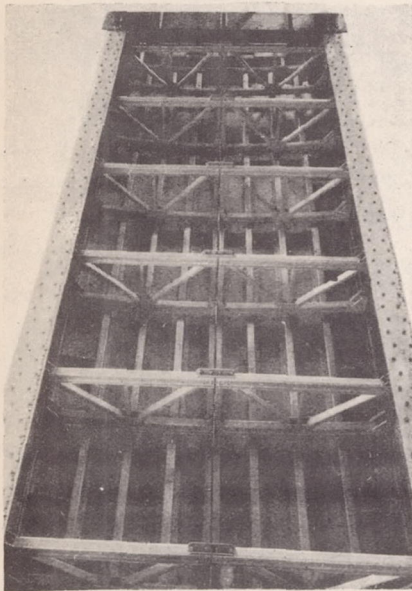


Figure 8.- Interior view of experimental wing.

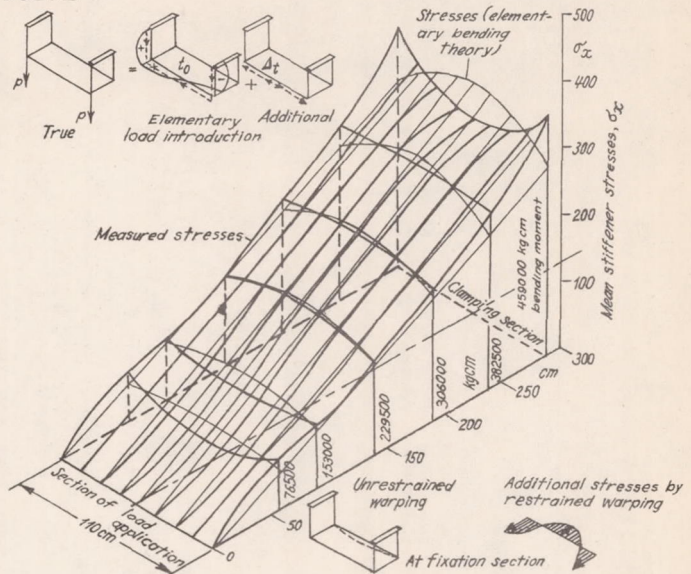
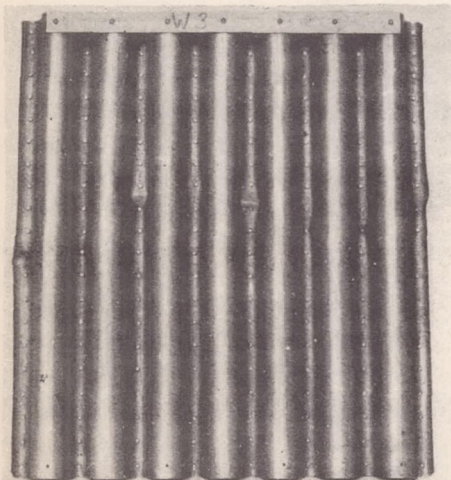
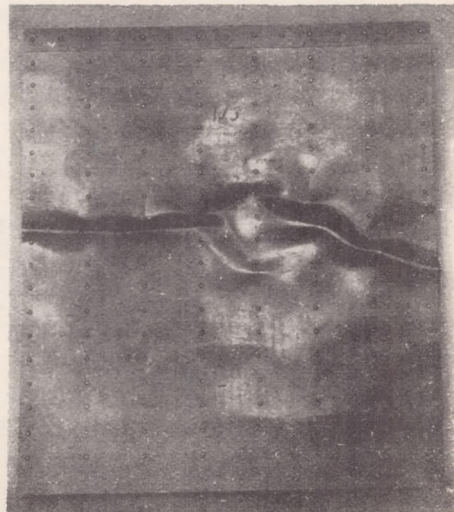


Figure 10.- Theoretical and experimental stress distribution in shell wing under applied transverse loads.



(a) View from corrugated side.



(b) View from smooth side

Figure 11.- Failure of panel with corrugated sheet stiffener.

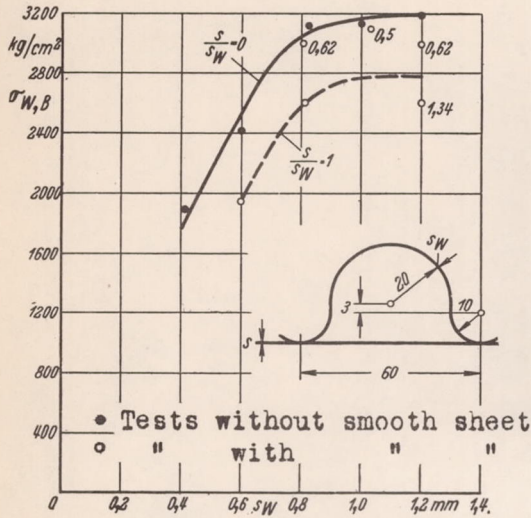


Figure 12.- Failing stress $\sigma_{W,B}$ of corrugated sheet for different thickness ratios of smooth and corrugated sheet.

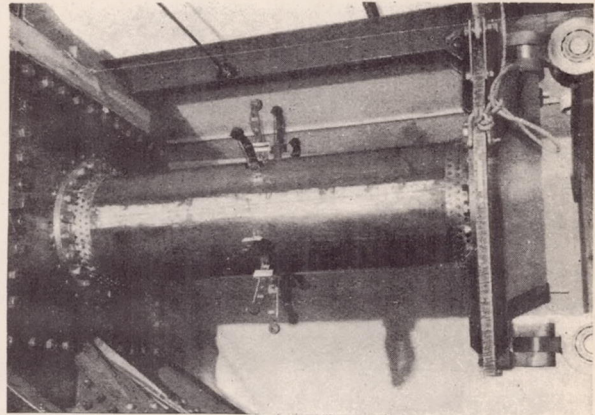
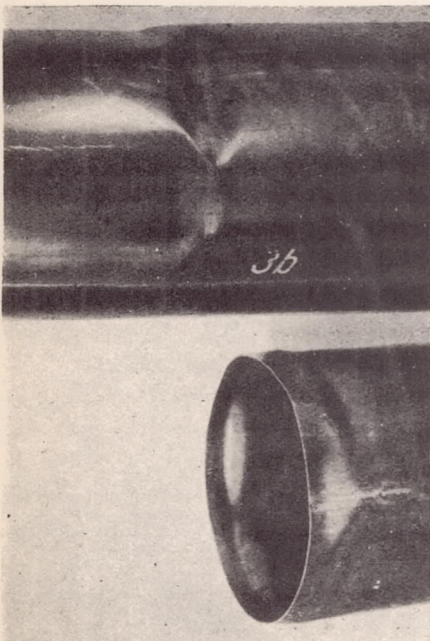


Figure 13.- Partial view of set-up for testing tubular spars in bending and torsion (specimen $d/s = 220$).



a. In pure bending
b. " " compression
Figure 14.- Failure of tubular spar.

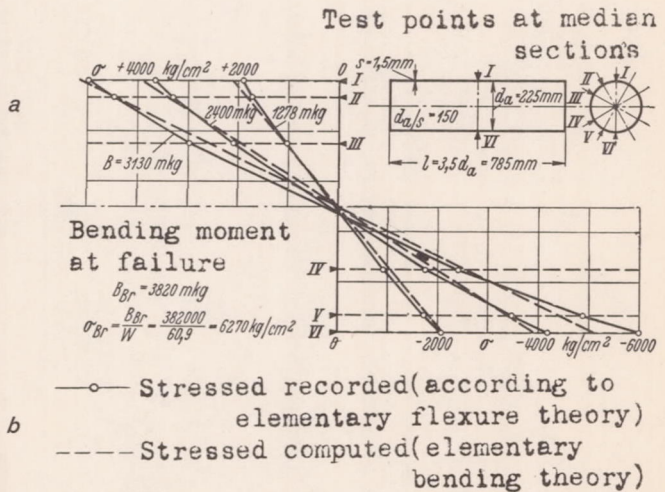


Figure 15.- Stress distribution of tubular spar in pure bending.